

Simulation of tensile performance of fiber reinforced cementitious composite with fracture mechanics model

J. Zhang

Department of Civil Engineering, Tsinghua University, Beijing, China

C. K.Y. Leung

Department of Civil and Environmental Engineering, HKUST, Hong Kong, China

Y. Gao

Department of Civil Engineering, Tsinghua University, Beijing, China

ABSTRACT: Uniaxial tensile performance of fiber reinforced cementitious composite is simulated based on fracture mechanics criteria, with the specific objective to study the phenomena of strain-hardening and multiple cracking under direct tension. In the model, instead of describing the matrix fracture resistance by a single parameter at the crack tip, we separate it into two parts, a crack tip toughness (KIC_M) and a tension softening curve representing the interlocking effect of aggregates. The latter is added to the fiber bridging stress to come up with the overall bridging stress vs crack opening relation for fracture analysis. To analyze crack propagation, a superposition method is employed to calculate the stress intensity factor at the crack tip resulted from both the applied load and the crack bridging stress. For a particular crack size, the corresponding load is calculated as the value when KIC_M is reached at the crack tip. Using the model, the effects of various material parameters, including matrix toughness, initial flow size, fiber content and specimen geometry on the tensile performances are investigated. The requirements for tensile strain-hardening and multiple cracking are analyzed and possible methods for material performance optimization are discussed.

1 INTRODUCTION

Concrete is a typical brittle material where first cracking in tension is accompanied by immediate localization of deformation followed by decreasing load. In normal reinforced concrete structures, as the stress reaches the tensile strength of concrete under mechanical and/or environmental loads, a small number of widely spaced discrete cracks will form and the crack width quickly opens to a macroscopically visible level. The formation of widely opened cracks allows water and other chemical agents, such as deicing salt, to go through the cover layer to come into contact with the reinforcements. The durability of the concrete structure is then significantly affected. Many methods have been proposed to improve the durability of concrete structures in the past, but most focus on the transport properties of un-cracked concrete, with little attention paid to the control of cracks. To prevent the rapid penetration of water and corrosive chemicals through cracks, a fundamental approach to reduce the crack width in concrete during its service stage has to be developed (Lepech et al. 2006).

In recent years, a class of high performance fiber

reinforced cementitious composite, called Engineered Cementitious Composites (ECC), with an ultimate strength higher than their first cracking strength and the formation of multiple cracking during the inelastic deformation process has been developed (Li, 2002). After first cracking, tensile load-carrying capacity continues to increase, resulting in strain-hardening accompanied by multiple cracking. For each individual crack, the crack width first increases steadily up a certain level and then stabilizes at a constant value. Further increase in strain capacity is resulted from the formation of additional cracks until the cracking reaches a saturated state with crack spacing limited by the stress transfer capability of the fibers. After that, a single crack localizes and the load slowly drops with increased deformation. Typically, strain localization occurs at a tensile strain of 3-5%, with crack spacing of 3-6mm and crack width around 60 μ m (Li, 2002). Cracks of such a small width will have little effect on the water permeability of the material (Wang, et al. 1997). With little degradation in transport properties under high deformation, the durability of the structure can be maintained.

The design criterion for ECC is first proposed by Li and Leung (Li & Leung, 1992) and further devel-

oped in subsequent investigations (Li 1993, Leung 1996, Kanda et al. 1999). To come up with the condition for multiple cracking to be achieved, fracture analysis is performed on a crack bridged by fibers. Also, in the analysis, the crack is taken to be propagating in an infinite space. In reality, however, an air void that is not bridged by fibers can serve as the crack initiator. In other words, the crack is initially not bridged by fibers, and the bridging effect becomes more and more significant as the crack grows in size. Also, when the crack approaches the boundary of the specimen, the stress intensity due to both the applied load and the bridging stresses will vary significantly from that in the infinite domain. To take these effects into consideration, a new fracture mechanics model is proposed in this paper for the analysis of cracking in fiber reinforced cementitious composites.

The field of fracture mechanics originated in the 1920's with A. A. Griffith's work on fracture of brittle materials such as glass (Griffith 1921). Its most significant applications, however, have been for the control of brittle fracture and fatigue failure of metallic structures such as pressure vessels, airplanes, ships etc. In the last thirty years, many attempts have been made to apply the fracture mechanics concept to cement-based composites, including mortar, concrete and fiber reinforced concrete (FRC). Pervious studies on this class of materials have shown that a relative large microcracking zone, referred to as the fracture process zone where material behaves nonlinearly, exists adjacent to the crack front. Since the size of the zone is not small in comparison to the size of the member, the stress distribution within the zone has to be considered explicitly in the analysis of crack propagation. Two major kinds of model have been developed to describe the fracture process zone, including (1) the fictitious crack model (FCM) proposed by Hillerborg et al. (1976) and (2) the crack band theory proposed by Bazant et al. (1983). The former approach models the process zone as part of the crack but with bridging stress governed by the crack opening. In other words, the behavior of the process zone follows a certain crack bridging law. The latter imagines the process zone to exist within a finite band width in which the microcracks are uniformly distributed and the behavior after cracking can be described by a softening stress-strain relationship. In the literature, these models are sometimes referred to as cohesive models, or fracture process models. In the present work, FCM will be applied to account for the behavior of the process zone.

In the past, researchers had attempted to use classical LEFM and crack bridging law to analyze the crack propagation in materials which exhibit crack bridging, such as fiber reinforced ceramics and fiber reinforced concrete (Cox et al. 1991, Li et al. 1986). Since a sharp crack tip is still envisaged to be present

at the leading edge of the process zone in concrete, reinforced ceramics, or even reinforced metals, it is more realistic to assume the bridging force within the process zone to reduce the net stress intensity factor at the crack tip, but a non-zero stress intensity still exists (Cox et al. 1991, Li et al. 1986). The crack propagating criterion of linear elastic fracture mechanics then remains applicable to the above materials, as long as the contribution of the process zone to the crack tip stress intensity factor is explicitly incorporated.

In the present paper, mode I crack propagation in fiber reinforced cementitious composite is simulated based on fracture mechanics criteria, with the specific objective to study the condition for multiple cracking to occur under direct tension. Compared to existing models on the propagation of bridged cracks in fiber materials, there are three additional considerations in this work. Firstly, we assume cracks to initiate from internal defects (such as entrapped air bubbles) which are not bridged by fibers. Therefore, fiber bridging effects do not affect crack initiation but come into play during the propagation of cracks. Secondly, when multiple cracking occurs, the crack opening is normally controlled to very small values. Instead of describing the matrix fracture resistance by a single parameter at the crack tip, we separate it into two parts, the crack tip toughness ($K_{IC,M}$) and a tension softening curve representing the interlocking effect of aggregates. The latter is added to the fiber bridging stress to come up with the overall bridging stress with crack opening relation for fracture analysis. Thirdly, the finite width of the member is considered in the analysis. To analyze crack propagation, a superposition method is employed to calculate the stress intensity factor at the crack tip resulted from both the applied load and the crack bridging stress. For a particular crack size, the corresponding load is calculated as the value when $K_{IC,M}$ is reached at the crack tip. Using the model, the effects of various material parameters, including matrix toughness ($K_{IC,M}$), size of initial unbridged flaw and fiber content on the tensile performances are investigated. The requirements for tensile strain-hardening and multiple cracking are analyzed and possible methods for material performance optimization are discussed.

2 PROBLEM FORMULATION

In the present model, the fine aggregates in the matrix are viewed as bridging elements and a fracture toughness calculated from the cracking load for a given specimen geometry (such as a single notched

beam under bending load) serves as the criteria of crack propagation. In other words, crack propagation occurs when:

$$K_{tip} = K_{IC} \quad (1)$$

where K_{IC} is the fracture toughness of material and K_{tip} is the net stress intensity resulting from both the applied load and the bridging stresses. Thus, the problem reduces to obtaining the crack tip stress intensity factor due to the external force and crack bridging stresses respectively.

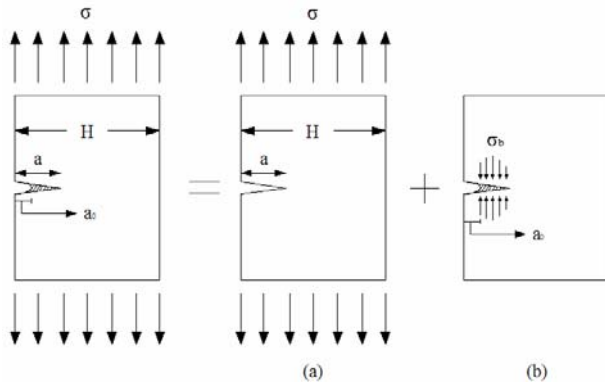


Figure 1. Principle of superposition in edged specimen under uniaxial tensile stress and crack bridging stress.

As an example, a single edge notch specimen under uniaxial tension load will be considered. Figure 1 shows a single edge notch specimen with initial flaw size (unbridged crack), a_0 , bridged crack length, a and external tensile load, σ_a . The bridging stress acting on the crack surface along the cracking section is σ_b , which is a function of crack opening. Based on the superposition scheme shown in Figure 1, the crack tip stress intensity factor can be obtained by summing the contributions K_a of external load and K_b of the bridging force (Zhang & Li 2004), i.e.

$$K_{tip} = K_a + K_b \quad (2)$$

K_a can be calculated as the stress intensity factor due to the presence of constant stress σ_a along the whole crack (including the bridged part). Under tensile load P , $\sigma_a = P/bt$, where b and t are depth and width of the specimen respectively. Then K_a is calculated by

$$K_a = 2 \int_0^a G(x, a, h) \sigma_a dx \quad (3)$$

where $G(x, a, h)$ is the weight function representing the contribution of a unit force on the crack surface to the crack tip stress intensity factor and is specific to specimen geometry and crack configuration (Tada 1985). For a single edge notch specimen under uniaxial tension, it is given by

$$G(x, a, h) = \frac{h_1(x/a, a/h)}{\sqrt{\pi a (1 - x^2/a^2)^{1/2}}} \quad (4)$$

where

$$h_1(x/a, a/h) = \frac{g(x/a, a/h)}{(1 - a/h)^{3/2}} \quad (5)$$

with $g(x/a, a/h)$ defined by

$$g(r, s) = g_1(s) + r g_2(s) + r^2 g_3(s) + r^3 g_4(s)$$

$$g_1(s) = 0.46 + 3.06s + 0.84(1-s)^5 + 0.66s^2(1-s)^2$$

$$g_2(s) = -3.52s^2$$

$$g_3(s) = 6.17 - 28.22s + 34.54s^2 - 14.39s^3 - (1-s)^{3/2} - 5.88(1-s)^5 - 2.64s^2(1-s)^2$$

$$g_4(s) = -6.63 + 25.16s - 31.04s^2 + 14.41s^3 + 2(1-s)^{3/2} + 5.04(1-s)^5 + 1.98s^2(1-s)^2$$

Similar to the above, the contribution K_b of the bridging force to the crack tip stress intensity factor can be given by

$$K_b = -2 \int_0^a G(x, a, h) \sigma_b(w(x)) dx \quad (6)$$

The fundamental material property of the crack bridging law $\sigma_b(w(x))$ will be given as an material property input. Thus, for a given geometry, loading model, crack configuration and crack bridging law, if the crack profile, $w(x)$, $x \in (0, a)$ is known, K_{tip} can be calculated by the above equations. When K_{tip} achieves the K_{IC-M} value, crack starts to propagate. Now the remaining problem is to find the crack profile for a given crack length. Following the standard derivation outlined in Cox and Marshall (1991), the crack opening profile $w(x)$ can be related to the applied tensile stress σ_a and bridging stress $\sigma_b(w(x))$ as

$$\delta(x) = \frac{8}{E} \int_x^a \left\{ \int_0^{a'} G(x', a', h) [\sigma_a - \sigma_b(x')] dx' \right\} G(x, a', h) da' \quad (7)$$

Thus, for a given crack length, a ($a \geq a_0$, a_0 is the initial unbridged flaw size), solving equations (1), (2) and (7) numerically, the critical external load capacity σ_a and crack profile $w(x)$ can be obtained.

3 NUMERICAL METHOD

Instead of solving the above equations by integration during iteration towards self-consistency to $w(x)$, the problem can be solved in the matrix form. With reference to the single edge notch specimen shown in Figure 2, a number of nodes are distributed along the potential fracture line. The opening and closing stresses acting on the crack surface are replaced by nodal forces that are governed by the external tensile load and the crack opening displacement according to the stress-crack opening relationship respectively. When the fracture toughness of cement matrix is

reached at the crack tip, the node is split into two nodes and a pair of opposite forces is imposed on these two nodes. Assume the node number of crack tip is $m+1$, the equation of (2) and (7) can then be expressed into the matrix form as:

$$\begin{aligned} K_{ip} &= \sum_{i=1}^m 2G(x_j, a, h)(P_j - F_j) \\ &= \sum_{j=1}^m k_{jK}(P_j - F_j) \end{aligned} \quad (8)$$

$$\begin{aligned} w_i &= \frac{8}{E} \sum_{i=i}^m \sum_{j=1}^i G(x'_j, a', h)G(x, a'_i, h)\Delta l_i(P_j - F_j) \\ &= \sum_{j=1}^m k_{jw}(P_j - F_j) \end{aligned} \quad (9)$$

where k_{iK} and k_{iw} are the influencing factors of external load and/or fictitious force on the crack tip stress intensity factor and crack opening respectively. F_i can be related to w_i by

$$F_i = \frac{\sigma_{fc}}{1 + \left(\frac{w_i}{w_0}\right)^p} B\Delta l_i + \sigma_0 \left[2\left(\frac{w_i}{w^*}\right)^{1/2} - \frac{w_i}{w^*} \right] B\Delta l_i \quad (10)$$

Detailed description of the above relation and the explanation of the parameters will be given in the next section. For a given crack length, a and stress crack width relation, by solving equations (8), (9) and (10), the critical external load capacity σ_a , fictitious force F_i and crack profile $w(x)$ are obtained. The crack mouth opening displacement (CMOD) can be calculated from equation (9) as well. The conventional tensile stress-deformation diagram, such as stress-crack length and stress-crack mouth opening displacement (CMOD) curves can then be obtained by the above numerical procedure.

4 MATERIAL PARAMETERS FOR MODEL INPUT

The parameters used in the model include fracture toughness of matrix K_{IC_M} , cracking strength σ_{fc} , initial unbridged flaw size a_0 and crack bridging law (or stress-crack opening relationship).

(1) Fracture toughness and cracking strength of matrix.

The toughness of cement matrix is a critical material property in the simulation of crack propagation.

In the past, some studies had been carried out to determine the fracture toughness of cement paste as well as mortar and concrete (Higgins et al. 1976, Naus et al. 1969). In these studies, the contributions

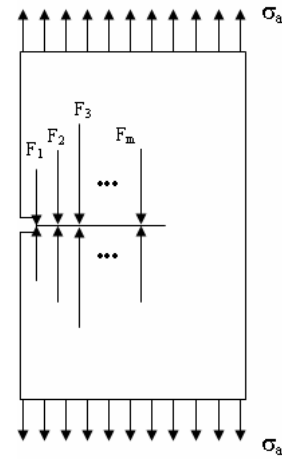


Figure 2. Finite element nodes and fictitious force on node along the potential fracture line.

of the process zone is included in calculating the fracture toughness, i.e. the peak load in the load-CMOD curves is used as the critical load for K_{IC} calculation. Therefore the measured value of K_{IC} is strongly influenced by the content of aggregates and is size dependent. However, if the contribution of the process zone is considered in the crack bridging law, then the fracture toughness of cement paste or mortar as well as concrete will be a constant, independent of specimen size. In this case, the critical load at which crack starts to propagate, i.e. the starting point of nonlinearity in the load-CMOD curve, should be used for fracture toughness calculation (Zhang & Leung & Cheung 2006, Zhang & Leung & Xu 2009a).

In addition, the cracking strength defined as the stress level at which the initial crack starts to propagate is the beginning point of the crack bridging law, which is required in the model calculation. Both the cracking strength and fracture toughness can be determined directly from experiments. For a pre-notched beam under bending load, according to the elastic theory, the CMOD and external load (P) obeys a linear relationship before the initiation of cracking. After initial cracking, the linear relationship between P and CMOD no longer exists. Thus the cracking load, P_{fc} can be determined by the point where the P -CMOD curve deviates from the initial linear portion. This point is regarded as the transition point from the linear-elastic stage to the nonlinear-elastic stage, in which a fictitious crack starts to develop. Typical graphs illustrating the determination of cracking load from three-point bending test on notched beam is shown in Figure 3. Based on the P_{fc} value, the corresponding cracking strength, σ_{fc} , is calculated from a finite element analysis that takes the notch effect into account. At the same time, fracture toughness K_{IC_M} is calculated also from P_{fc} through classical fracture mechanics theory. Based on test results provided in (Zhang et al. 2009b), the relationship between cracking strength and fracture toughness of PVA fiber reinforced cementitious

composites can be expressed as:

$$\sigma_{fc} = 25.78K_{IC-M} \quad (11)$$

where σ_{fc} is in the unit of MPa and K_{IC} is in the unit of $\text{MPam}^{1/2}$. In the present paper, the effect of K_{IC-M} and/or cracking strength on the composite tensile performance is investigated by varying K_{IC-M} from $0.05\text{MPam}^{1/2}$ to $0.20\text{MPam}^{1/2}$, and the corresponding σ_{fc} changes from 1.3MPa to 5.2MPa.

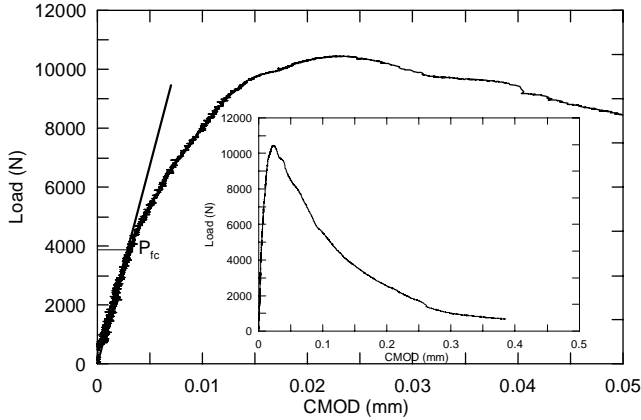


Figure 3. Determination of cracking load from bending test.

(2) Crack bridging law

As a fundamental material property, crack bridging laws of cementitious composites, such as mortar, concrete and fiber reinforced cement composites have been investigated both experimentally and theoretically during recent years. The experimental results show that the shape of stress-crack width curve of fiber reinforced cement composite is complex and greatly influenced by the type and amount of fiber used (Stang et al. 1992). A micromechanics-based model for stress-crack width relationship of FRC materials has been developed by Li et al. (1993). The model provides a basic understanding of the influence of micro-parameters on the shape of the stress-crack width curve and is especially useful for material design. In this work, the micromechanics-based model developed by Li et al. (1993) is used as the crack bridging law ($\sigma-w$), which is given by:

$$\begin{cases} \sigma_f(w) = \sigma_0 \left[2 \left(\frac{w}{w^*} \right)^{\frac{1}{2}} - \frac{w}{w^*} \right] & \text{for } 0 \leq w \leq w^* \\ \sigma_f(w) = \sigma_0 \left[1 - \frac{2}{L_f} (w - w^*) \right]^2 & \text{for } w^* \leq w \leq \frac{L_f}{2} \end{cases} \quad (12)$$

where $\sigma_0 = \frac{g \tau V_f L_f}{2 d_f}$, $w^* = \frac{\alpha L_f^2}{(1+\eta) E_f d_f}$, $g = \frac{2}{4+f^2} (1+e^{\eta/2})$. In the equations, d_f , L_f , V_f , E_f stand for fiber diameter, length, volume fraction and elastic modulus respectively. τ is fiber/matrix bond strength. f is snubbing coefficient that reflecting the effect of inclination an-

gle. $\eta = V_f E_f / V_m E_m$ and V_m , E_m are matrix volume fraction and matrix elastic modulus. Typical PVA fiber and fiber/matrix interfacial parameters used in the model are listed in Table 1.

Apart from fiber bridging, matrix itself also exhibits bridging action due to the presence of fine aggregates. Due to the lack of a good physical model, an empirical model proposed by Stang et al. (1992) is used for matrix bridging calculation in the present work. In the model, the matrix bridging stress σ_m is expressed as a function of the crack opening w as:

$$\sigma_m = \frac{\sigma_{fc}}{1 + \left(\frac{w}{w_0} \right)^p} \quad (13)$$

where σ_{fc} is matrix bridging stress at $w=0$, i.e. matrix cracking strength. The parameter p describes the shape of the softening curve with increase of crack opening. The parameter w_0 corresponds to the crack opening when the stress has dropped to half of σ_{fc} . For concrete, good fitting of experimental results can be obtained with $p=1.2$ and $w_0=0.015\text{mm}$ (Stang et al. 1992). Because the present work is focused on the matrix without coarse aggregate, a smaller value of w_0 is used ($w_0=0.010\text{mm}$). The total crack bridging of the composite can be obtained by summing (12) and (13) as shown in (10). Typical stress-crack width relationship of PVA fiber reinforced cement composite with the separate components is shown in Figure 4.

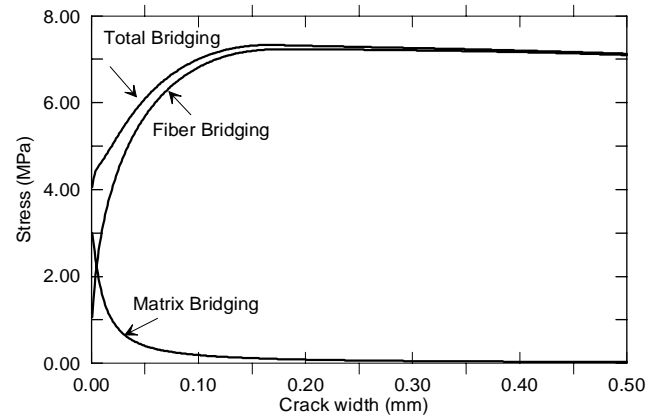


Figure 4. Crack bridging in fiber reinforced cementitious composite.

(3) Initial unbridged flaw size

In cement matrix, flaws are typically the sources where cracks are initiated. Most flaws inherent from the mixing process have sizes below 1-2mm, and their existence may considerably reduce the cracking strength (Zhang & Li 2004). In the model, the initial flaw is an equivalent crack resulted from defects at the surface of specimen. These defects might result

from air voids, aggregate/cement paste interfacial cracks and other possible damage in the material (e.g. shrinkage cracks). In the present study, a set of initial unbridged flaw size a_0 within 0.125 to 1.25 mm is used in the model calculation to investigate their effects on tensile performance.

5 RESULTS AND DISCUSSION

In this section, the tensile performance of a single edge specimen made of PVA fiber reinforced cementitious composites is simulated with the developed model. The influence of fracture toughness of matrix K_{IC_M} (with the effect of σ_{fc} also involved), fiber bridging stress reflected by fiber content as well as initial unbridged flaw size a_0 on the tensile performance of the composite are presented and discussed. The related material parameters used in the model are listed in Table 1 where constant fiber/matrix interfacial bond strength is assumed despite the variation in matrix strength and toughness.

Table 1. Parameters of matrix, fiber and fiber/matrix interface.

Tensile strength (MPa)	E_f (GPa)	d_f (mm)	L_f (mm)	E_m (GPa)	τ (MPa)	f
1620	42.8	0.039	12	20.0	2.0	0.8

Effect of fracture toughness

Figures 5a and 5b show the effect of matrix toughness K_{IC_M} on the tensile behavior, in terms of tensile stress versus crack length and crack mouth opening relations respectively. The simulation results are for a single edged specimen with a constant unbridged initial notch of 0.25mm. From these figures, it can be observed that the global tensile load carrying capacity for a fixed crack bridging law increases with the increase of K_{IC_M} at the initial stage of crack development. After the crack length achieving about 80% of the total specimen width, all curves start to converge to the same loading capacity, which is the maximum fiber bridging capacity. With increase of matrix toughness, the tensile stress versus crack length relation is gradually changed from a monotonic increasing trend to an initially decreasing trend followed by increasing stress. This behavior can also be found in the curves of tensile stress versus crack mouth opening (Fig. 5b). The rate of stress decrease at the initial stage of crack propagation is reduced with decreasing matrix toughness and finally changes to a trend with monotonic increasing stress as matrix toughness is reduced to a certain value, which is $K_{IC_M}=0.05\text{MPam}^{1/2}$ in this case. The increase of tensile strength with crack length shows the possibility of multiple-cracking in the material under tension, which of great interest for material ductility improvement. If the cracking stress is blow the peak

tensile strength and the local stress at the maximum crack opening along the crack length is also lower than the peak bridging stress, the composite has strain-hardening potential, i.e. there exists a margin of load carrying capacity for developing sequential multiple cracking.

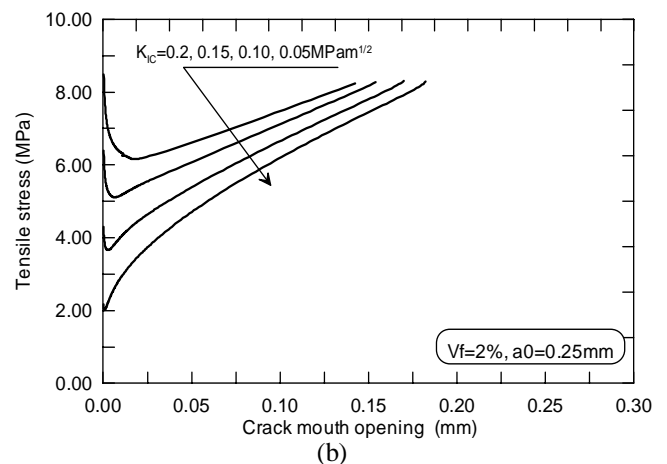
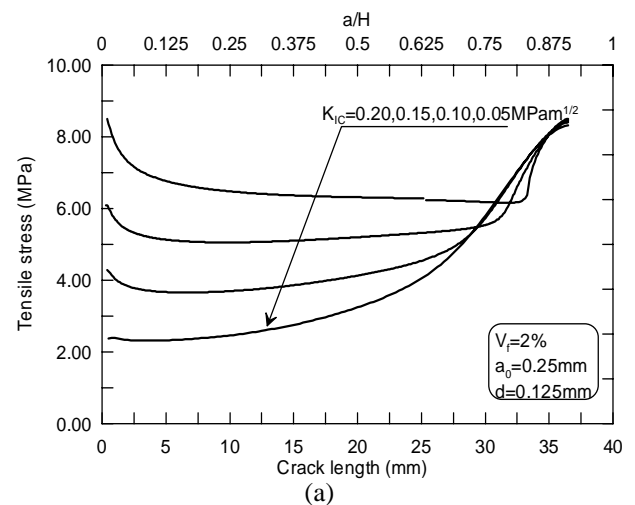


Figure 5. Tensile stress versus crack length (a) and crack mouth opening (b) curves of edged specimen with different matrix toughness.

The results present in Figure 5 clearly show that the lower the matrix fracture toughness, the higher the likelihood of multiple cracking. This is consistent with the experimental results that ECC with higher matrix strength has a lower tensile strain capacity (Zhang et al. 2009c). On the other hand, the above results also indicate that the reduction of matrix toughness will help to reduce the stress jump which occurs during loading, which is commonly observed in tensile tests (Zhang et al. 2009c). It needs to be noted that the fiber/matrix interfacial bond strength and bond related parameters are assumed to be constant even when K_{IC_M} is varying. This assumption may be reasonable because previous experimental results shown that the effect of matrix proportion on the fiber/matrix bond strength of PVA fiber reinforced cementitious composite is limited due to the strong chemical bond between PVA fiber and cement matrix (Li et al. 2002).

Effect of fiber bridging

Most high performance fiber reinforced cementitious composites are reinforced by short discontinuous fibers. Crack bridging provided by fibers in the composite is one of the most important factors governing the macroscopic mechanical properties of the composite. Figures 6a and 6b display the effect of fiber volume content (V_f), which governs fiber bridging, on the tensile stress versus crack length and crack mouth opening (CMOD) diagrams respectively. Figure 7 presents the corresponding stress-crack opening relationship of the composites with different fiber content. In the calculation, $K_{IC,M}=0.1\text{MPam}^{1/2}$ and fiber parameters listed in Table 1 were used. Fiber volume of 0%, 1.0%, and 2.0% were used in the simulation. According to the results, for the given PVA fiber and related fiber/matrix interfacial parameters, as fiber content reaches 2%, the composite starts to show strain-hardening behavior. By contrast, as fiber content is lower than 2%, strain softening under tensile load can be expected. Clearly, the requirement on fiber bridging, represented by fiber content, is critical for strain-hardening achievement. For given matrix, fiber and fiber/matrix interfacial parameters, the volume of fiber needed for strain-hardening and multiple cracking performance of the composite can be obtained through model simulation.

As an example to illustrate fiber bridging, the crack profile and corresponding stress distribution along the crack length at different crack propagation stage (reflected by crack length) are shown in Figures 8 and 9 for fiber content of 0 and 2% respectively. In the calculation, $K_{IC,M}=0.10\text{MPam}^{1/2}$ and initial flaw size $a_0=0.25\text{mm}$ were assumed. Differences in the crack shape as well as stress distribution along the crack can be observed for the two cases. When there is no fiber reinforcement, the crack opening increases monotonically with distance from the crack tip, so maximum and minimum crack opening occur at crack mouth and tip respectively. The stress distribution along the crack shows obvious softening with increase of crack opening. For the composite with 2% fiber addition, at initial stage of crack growth, for crack

length less than 30mm, the crack opening along the crack length increases monotonically with distance from the crack tip. As crack length increases to a certain level, say about 80% of the specimen width, the crack profile shows an arc shape with maximum crack opening occurring near the center of the crack. The corresponded stress distribution along the crack length displayed in Figure 9b is also interesting. For crack length over 25mm, the stress value along the crack becomes almost constant except for a small zone near the crack tip and the stress increases with increasing crack opening. This is similar to the so-

called steady-state cracking that is the basic requirement for material strain-hardening (Li & Leung, 1992, Li 1993, Leung 1996). However, steady-state here refers to the almost constant stress distribution along the crack, rather than the constant crack opening along the crack length described in former models (Li & Leung 1992, Li 1993, Leung 1996). The present work shows that an arc shape crack profile may be resulted even under steady-state and strain-hardening condition.

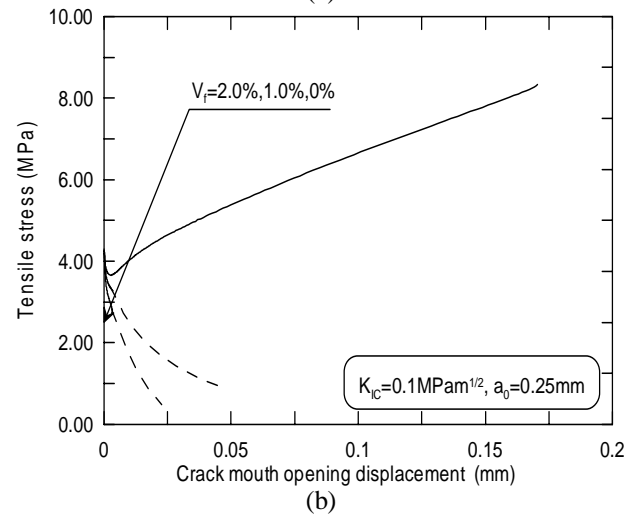
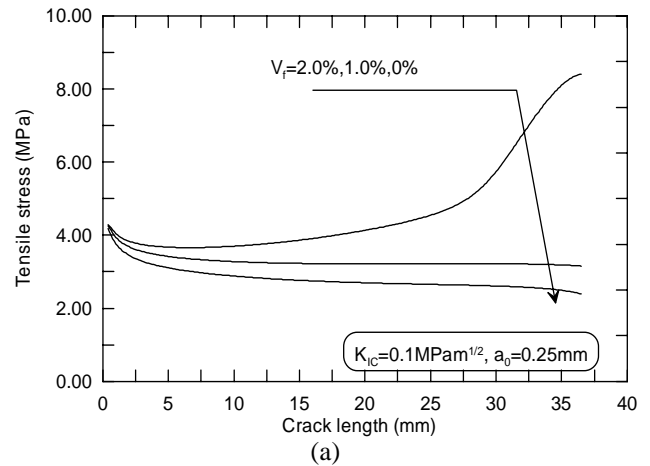


Figure 6. Tensile stress versus crack length (a) and crack mouth opening (b) curves of edged specimen with different matrix toughness.

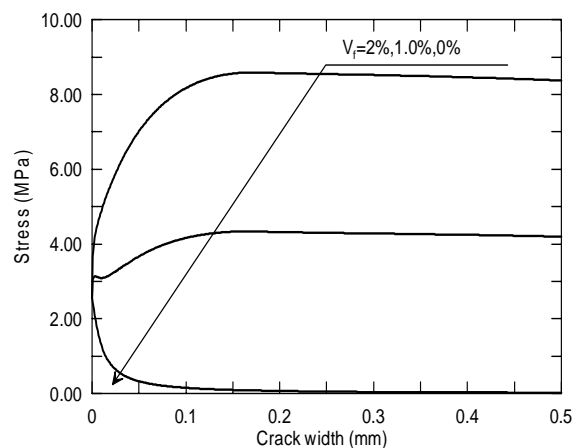


Figure 7. Stress crack opening relationship of the composite with different fiber content.

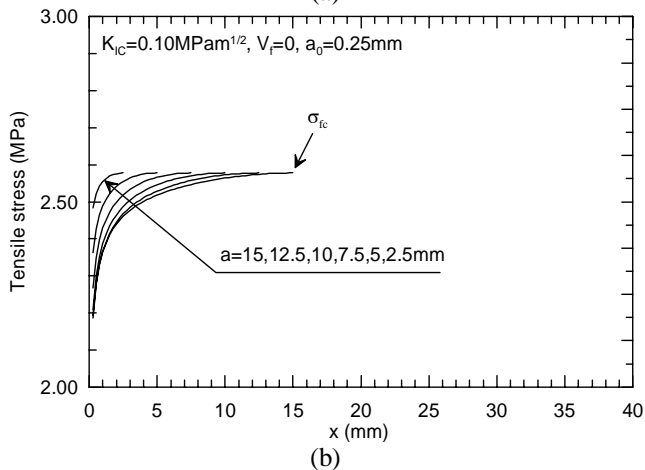
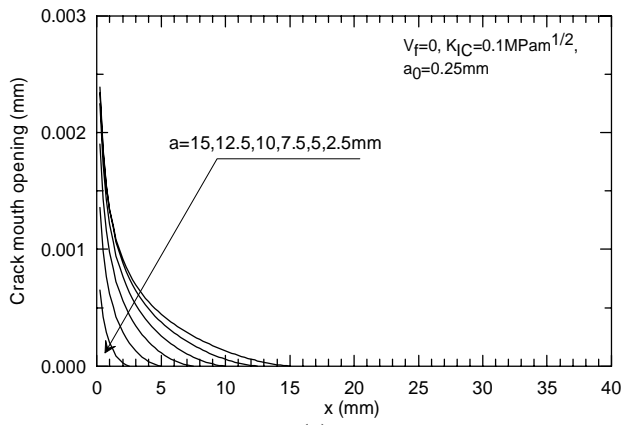


Figure 8. Crack profiles (a) and stress distribution (b) at different crack length of edged specimen with $V_f=0$.

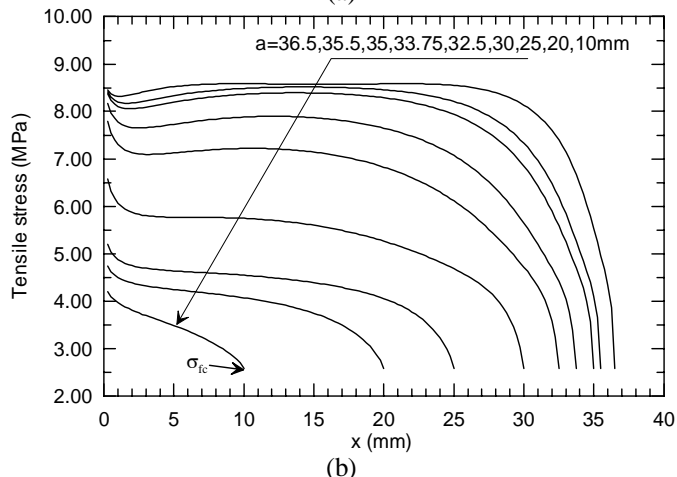
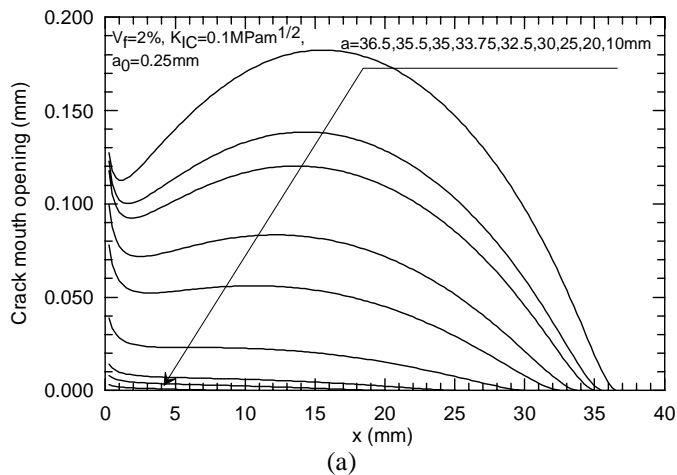


Figure 9. Crack profiles (a) and stress distribution (b) at different crack length of edged specimen with $V_f=2\%$.

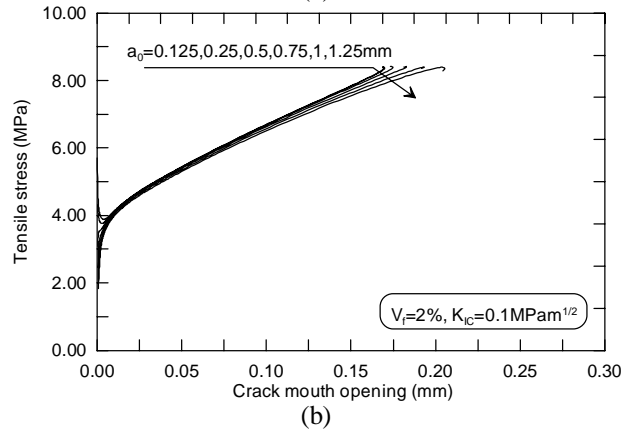
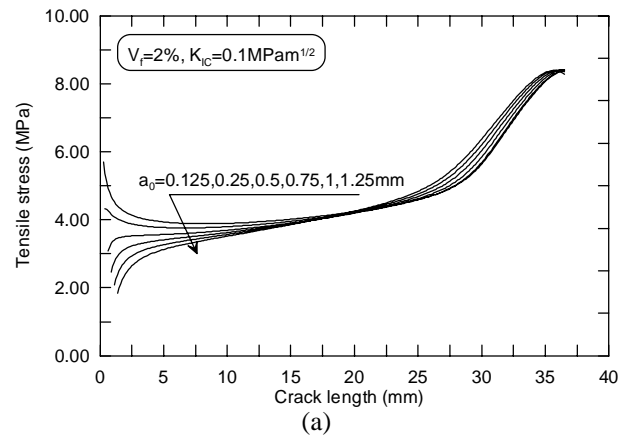


Figure 10. Tensile stress versus crack length (a) crack mouth opening (b) curves of edged specimen with different initial flaw size.

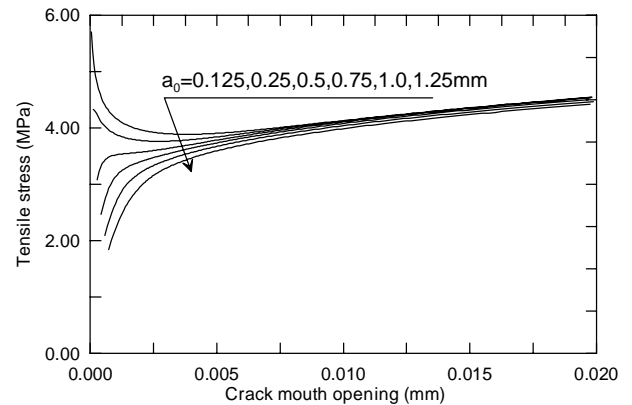


Figure 11. Close up on the tensile stress-crack mouth opening curves of edged specimen with different initial flaw size.

Effect of initial unbridged flaw size

Figures 10a and 10b show the effect of initial unbridged flaw size (a_0) on the tensile stress versus crack length and crack mouth opening (CMOD) relations respectively. Figure 11 shows the close up of the stress- CMOD curves to see the beginning parts more clearly. In the calculation, $V_f=2\%$ and $K_{IC-M}=0.1\text{MPam}^{1/2}$ were used. From these curves, it can be seen that for fixed K_{IC-M} and crack bridging law, a trend similar to

the effect of K_{IC-M} is also found for a_0 changing from 0.125mm to 1.25mm. The larger the initial flaw size a_0 , the lower the first cracking load. This indicates that the enlargement of the initial unbridged

flaw will enhance the strain-hardening and multiple cracking potentials of the composite. This idea has already been used in the production of high ductility ECC by Li et al. (2006) and Wang et al. (2007), who introduced small plastic bubbles into the matrix to increase the tensile strain capacity. The number and size distribution of the initial unbridged flaw in matrix control the number of cracks that will form during strain hardening prior to reaching the peak bridging stress. Therefore, these two parameters will also govern the ultimate tensile strain capacity of the composite. Apparently, the unbridged flaws in matrix play an important role in multiple cracking performance of the composite. High ductility is closely associated with the density of multiple cracks, and saturated multiple cracking can only be reached when a sufficient number of flaws exist. The inherent flaws in cementitious matrix, such as pores and weak boundaries between phases possess a random nature (Wang et al. 2007). The uniformity of the flaws will influence the number of cracks occurring under a certain tensile load level. When more flaws are having the same or similar size, the higher will be the number of cracks occurring under a give load. Thus, the composite ductility can be improved by manually adding small solid particles which has relative weak interfacial bond strength to matrix. By incorporating particles of similar size to develop a very narrow distribution of the initial flaw size in the matrix, more cracks will form under slowly increased loading to enhance the tensile ductility.

6 CONCLUSIONS

This article presents a theoretical study on the model I crack propagation in cementitious composite with the specific objective to study the phenomena of strain-hardening and multiple cracking under direct tension. A fracture mechanics based model for crack propagation simulation of fiber reinforced cementitious composite under direct tension is developed. The model assumes cracks to initiate from internal defects which are not bridged by fibers initially. In the model, instead of describing the matrix fracture resistance by a single parameter at the crack tip, we separate it into two parts, a crack tip toughness and a tension softening curve representing the interlocking effect of aggregates. The latter is added to the fiber bridging stress to come up with the overall bridging stress with crack opening relation for fracture analysis.

Using the model, the effects of various material parameters, including matrix toughness, initial flaw size in matrix and fiber content on the tensile performance are investigated. With the model results, the transition from tension softening to strain hardening and multiple cracking behavior can be quantified. Lower fracture toughness of matrix, larger initial

flaw size and improved crack bridging with a higher fiber content will enhance the possibility of strain-hardening and multiple cracking. While the general conclusions are similar to those from conventional theories, the present analysis is believed to provide a more accurate description of the cracking process in fiber reinforced cementitious composites and give better estimates of the range of micro-parameters for the design of composites with pseudo-ductile behavior.

ACKNOWLEDGEMENTS

Support from the National Science Foundation of China (No.50878119) to Tsinghua University are gratefully acknowledged.

REFERENCES

- Bazant, Z.P. & Oh, B.H., 1983. Crack band theory for fracture of concrete. *Material and Structure*, 16:155-177.
- Cox, B.N. & Marshall, D.B. 1991. Stable and unstable solutions for bridged cracks in various specimens. *Acta Metall. Mater.*, 39 (4):579-589.
- Griffith, A.A., 1921. The phenomena of rupture and flow in solids. *Phil. Trans. Roy. Soc.*, series A221:163-168.
- Higgins, D.D. & Bailey, J.E. 1976. Fracture measurement on cement paste. *Journal of Materials Science*, 11:1995-2003.
- Hillerborg, A., Mod er, M. & Petersson, P-E. 1976. Analysis of crack formation and crack growth by means of fracture mechanics and finite elements, *Cem Concr Res*, 6:773-782.
- Kanda, T. & Li, V.C. 1999. A New Micromechanics Design Theory for Pseudo Strain Hardening Cementitious Composite, *ASCE J. of Engineering Mechanics*, 125:373-381.
- Lepech, M.D., Li, V.C., Lepech, M.D. & V.C. Li, 2006. Long Term Durability Performance of Engineered Cementitious Composites. *International Journal for Restoration of Buildings and Monuments*, 12(2):119-132.
- Leung, C.K.Y., 1996. Design Criteria for Pseudo-ductile Fiber Composites, *ASCE J. of Engineering Mechanics*, 122:10-18.
- Li V.C., Stang, H. & Krenchel, H., 1993. Micromechanics of crack bridging in fibre reinforced concrete, *Materials and Structures*, 26:486-494.
- Li, V. C. & Wang, S. 2006. Microstructure Variability and Macroscopic Composite Properties of High Performance Fiber Reinforced Cementitious Composites. *Probabilistic Engineering Mechanics*, 21 (3):201-206.
- Li, V. C., Wu, C., Wang, S., Ogawa, A. & Saito, T. 2002. Interface Tailoring for Strain-hardening PVA-ECC. *ACI Materials Journal*, 99 (5):463-472.
- Li, V.C. & Leung, C.K.Y. 1992. Steady State and Multiple Cracking of Short Random Fiber Composites", *ASCE J. of Engineering Mechanics*, 118:2246-2264.
- Li, V.C. & Liang, E. 1986. Fracture processes in concrete and fiber reinforced cementitious composites. *Journal of Engineering Mechanics*, 112 (6):566-586.
- Li, V.C. 1993. From Micromechanics to Structural Engineering--the Design of Cementitious Composites for Civil Engineering Applications. *JSCE J. of Strutural Mechanics and Earthquake Engineering*, 10:37-48.
- Li, V.C., 2002. Advances in ECC Research, ACI Special Pub-

- lication on Concrete: *Material Science to Applications*, SP 206-23:373-400.
- Naus, D.J. & Lott, J.L., 1969. Fracture toughness of portland cement concrete, *Journal of American Concrete Institute*, 481-489.
- Stang, H. & Aarre, T., 1992. Evaluation of crack width in FRC with conventional reinforcement. *Cement and Concrete Composites*, 14 (2):143-154.
- Tada, H., Paris, P.C. & Irwin, G., 1985. The stress analysis of cracks handbook, 2nd edn. Paris Prod. Inc., St Louis, Missouri.
- Wang, K. Wang, K., Jansen, D., Shah, S. & Karr, A., 1997. Permeability Study of Cracked Concrete, *Cement and Concrete Research*, 27:381-393.
- Wang, S. & Li, V. C., 2007. Engineered Cementitious Composites with High-volume Fly Ash. *ACI Material Journal*, 104 (3):233-241.
- Zhang J., Leung, C. K. Y. & Cheung, Y. N., 2006. Flexural Performance of Layered ECC-Concrete Composite Beam. *Composite Science and Technology*, 66 :1501-1512.
- Zhang J., Leung, C. K. Y. & Xu S., 2009a. Evaluation of Fracture Parameters of Concrete from Bending Test. *Materials and Structures*, In press.
- Zhang, J. & Li, V.C., 2004. Simulation of mode I crack propagation in fiber reinforced concrete by fracture mechanics. *Cement and Concrete Research*, 34:333-339.
- Zhang, J. Gong, C X., Ju, X.C. & Guo, Z L., 2009b. Flexural performance of high Ductile fiber reinforced cementitious composite. *Engineering Mechanics*, In press, (in Chinese).
- Zhang, J. Gong, C X., Zhang, M H. & Guo, Z L., 2009c. Engineered Cementitious Composite with Characteristic of Low Drying Shrinkage. *Cement and Concrete Research*, 39:303-312.